Supplement of Biogeosciences, 17, 1071–1085, 2020
https://doi.org/10.5194/bg-17-1071-2020-supplement

Biogeosciences Open Access EGU

Supplement of

Wintertime grassland dynamics may influence belowground biomass under climate change: a model analysis

Genki Katata et al.

Correspondence to: Genki Katata (genki.katata.mirai@vc.ibaraki.ac.jp)

Supplement

Description of newly modeled processes

SOLVEG is a one-dimensional multi-layer model that consists of four sub-models for the atmosphere near the surface, soil, vegetation, and radiation within the vegetation canopy (Fig. S1). Since full descriptions of the model are available in the papers by Nagai (2004), Katata (2009), Ota et al. (2013), and Katata and Ota (2017), we give details about cold processes newly modelled in the present study.

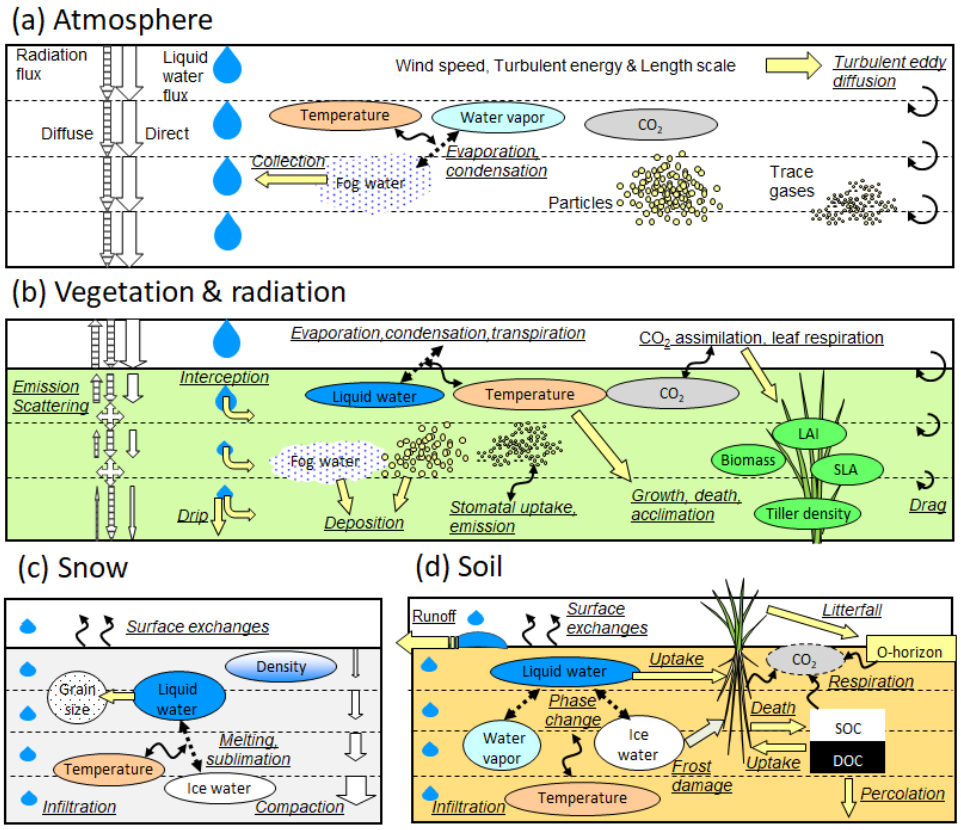

Fig. S1 Overview of key processes (underlined words) and variables for (a) atmosphere, (b) vegetation, radiation, (c) snow, and (d) soil submodels in SOLVEG. The part of the existing grass growth model of BASGRA is coupled in this study.

Modeling snow accumulation and melting processes

A multi-layer snow module is newly incorporated into the SOLVEG model. Most of the variables in the following equations are based on either the Community Land Model (CLM: Oleson *et al.*, 2010) or SNTHERM (Jordan 1991), while the model is unique in including the gravitational and capillary liquid water flows in unsaturated snow layer based on van Genuchten‘s concept of water flow in the unsaturated zone (c.f., Hirashima, Yamaguchi, Sati, & Lehning, 2010).

The temporal change in snow temperature T_{sn} (K) is expressed by the heat conduction equation based on Yamazaki (2001) as

$$C_{sn}\rho_{sn}\frac{\partial T_{sn}}{\partial t} = \frac{\partial}{\partial z}\left(\lambda_{sn}\frac{\partial T_{sn}}{\partial z}\right) - \frac{\partial I_n}{\partial z} - l_f E_{smel} - lE_{sb}, \qquad (1)$$

where C_{sn} and ρ_{sn} are the specific heat of snow (J kg^{-1} K^{-1}) and the density of the bulk snow (kg m^{-3}), respectively, λ_{sn} is the thermal conductivity of snow (Wm^{-1}K^{-1}), I_n is the net solar flux in the snow layer (W m^{-2}), l_f and l are the latent heats of fusion and sublimation (J kg^{-1}) , respectively, and E_{smel} is the melting or freezing rate in the snow layer (kg m^{-3} s^{-1}), and E_{sb} is the sublimation rate of water vapor from the snow layer (kg m^{-3} s^{-1}). I_n is calculated as:

$$(1-r)(1-A_b)S_{down}\,exp(-\mu z), \qquad (2)$$

where r is the absorptivity of solar radiation at the snow surface, A_b is the albedo of the snow surface as a sum of the direct and the diffuse visible and near-infrared solar and long-wave radiations (Wiscombe & Warren, 1980), and μ is the extinction coefficient of the solar radiation in the snow layer (Jordan, 1991).

The sublimation rate E_{sb} is calculated only at the snow surface by assuming that water vapor is saturated over the snow as:

$$E_{sb0} = \sigma_{sn}\rho c_{E0}|u|[q_{sat}(T_{sn0}) - q_r], \quad (3)$$

where σ_{sn} is the fractional area of snow cover parameterized using physical snow height (Essery, Morin, Lejeune, & Menard, 2013), ρ is the density of air (kg m^{-3}), c_{E0} is the bulk coefficient, $q_{sat}(T_{sn0})$ is the saturated specific humidity (kg kg^{-1}) at the snow surface temperature T_{sn0} (K), and $|u|$ and q_r are the horizontal wind speed (m s^{-1}) and specific humidity (kg kg^{-1}) at the lowest atmospheric layer, respectively.

Melting or freezing rate in the snow layer is calculated from snow temperature as:

$$E_{smel} = \frac{c_{sn}\rho_{sn}}{l_f}\frac{T_{sn}-T_m}{\partial t}, \quad (4)$$

where T_m is the melting point of 273.15 K. Using E_{smel}, the ice content in snow w_i (kg m^{-2}) at each snow layer is determined as:

$$\frac{\partial w_i}{\partial t} = -E_{smel}\Delta z, \quad (5)$$

where Δz is the snow layer thickness (m).

The mass balance equation for liquid water in the snow layer is given as:

$$\rho_w \frac{\partial \eta_{sw}}{\partial t} = \frac{\partial}{\partial z}\left(D_{sw}\frac{\partial \eta_{sw}}{\partial z} + K_{sw}\right) - E_{smel}, \quad (6)$$

where η_{sw} is the volumetric liquid water content (m^3 m^{-3}), D_{sw} is the liquid water diffusivity (m^2 s^{-1}), K_{sw} is the snow unsaturated hydraulic conductivity (m s^{-1}), and ρ_w is the density of liquid water (kg m^{-3}) in the snow layer. The equations for D_{sw} and K_{sw} are similar to those for soil

water content in the capillary region (Katata 2009), except for using the empirical parameters for the snow cover that are given by Hirashima *et al.* (2010).

Snow accumulation and compaction at each snow layer are modelled as:

$$\frac{1}{\Delta z}\frac{\partial \Delta z}{\partial t} = C_{snf} - C_{met} - C_{over} - C_{mel}, \quad (7)$$

$$C_{met} = c_1\, exp[-c_2(T_m - T_s) - c_3\, max(0, \rho_s - \rho_0)], \quad (8)$$

$$C_{over} = \frac{-P_s}{\eta_{sn}}, \quad (9)$$

$$C_{mel} = -\frac{1}{\Delta t} max\left(0, \frac{f_{ice} - f_{ice}^{+}}{f_{ice}}\right), \quad (10)$$

where C_{snf}, C_{met}, C_{over}, and C_{mel} are the change rates in Δz (s^{-1}) due to snowfall, metamorphism, overburden, and melting, respectively, and f_{ice} and f_{ice}^{+} the fractions of ice before and after the melting, respectively. C_{snf} is calculated as $S_f\, \rho_{fs}/\rho_w$, where S_f is the snowfall rate (mm s^{-1}) given by either the input data or the empirical equation using total rainfall rate and wet bulb temperature (Yamazaki 2001), and ρ_{fs} the fresh snow density (kg m^{-3}) obtained by Boone (2002). Values for the parameters in the above equations are given by Oleson *et al.* (2010).

Snow grain growth (i.e., change in grain size in the snow layer) is calculated based on Jordan (1991) as:

$$\frac{\partial d_{sn}}{\partial t} = \begin{cases} \frac{g_1 |U_v|}{d_{sn}} & \eta_{sw} = \eta_{swilt} \\ \frac{g_2}{d_{sn}}(\eta_{sw} + 0.05) & \eta_{swilt} < \eta_{sw} < 0.09, \\ 0.14\frac{g_2}{d_{sn}} & 0.09 < \eta_{sw} \end{cases} \quad (11)$$

where d_{sn} is the snow grain diameter (m), U_v the mass vapor flux in the snow layer (kg m^{-2} s^{-1}),

and g_1 and g_2 the parameters. The formulation of U_v and the values of g_1 and g_2 are given by Jordan (1991).

After the above calculations for temperature, liquid and ice water contents, and accumulation and compaction in snow, the number of snow layers is adjusted by either combining or subdividing layers (Jordan, 1991) to obtain the physical snow height.

Modeling freeze-thaw process in soil

In the soil module, freeze–thaw processes in soil are considered based on heat conduction and liquid water flow equations as follows:

$$C_s \rho_s \frac{\partial T_s}{\partial t} = \frac{\partial}{\partial z}\left(\lambda_s \frac{\partial T_s}{\partial z}\right) - lE_b - l_f E_{mel}, \quad (12)$$

$$\rho_w \frac{\partial \eta_w}{\partial t} = \frac{\partial}{\partial z}\left(D_w \frac{\partial \eta_w}{\partial z} + K\right) - E_b - E_{mel}, \quad (13)$$

where C_s and ρ_s are the specific heat of soil (J kg^{-1} K^{-1}) and the density of the bulk soil (kg m^{-3}), respectively, λ_s is the thermal conductivity of soil (W m^{-1} K^{-1}), l_f and l are the latent heat of fusion and sublimation (J kg^{-1}) , respectively, η_w is the volumetric soil water content (m^3 m^{-3}), D_w is the soil water diffusivity (m^2 s^{-1}), K is the unsaturated hydraulic conductivity (m s^{-1}), E_b is the evaporation or condensation or sublimation of soil water (kg m^{-2} s^{-1}), and E_{mel} is the melting or freezing rate in soil (kg m^{-3} s^{-1}). The soil water diffusivity D_w (m^2 s^{-1}) is expressed by:

$$D_w = K \frac{\partial \psi}{\partial \eta_w}, \quad (14)$$

where ψ is the water potential in the soil layer (m). ψ and K (m s^{-1}) in frozen soil are modeled based on the concept of freezing point depression (Zhang, Sun, & Xue, 2007):

$$\psi = \psi_{unfrozen}(1 + C_k\eta_i)^2, \quad (15)$$

$$K = K_{unfrozen}10^{-E_i\eta_i}, \quad (16)$$

where C_k and E_i are the empirical parameters, and $\psi_{unfrozen}$ and $K_{unfrozen}$ are the ψ and K in unfrozen soil described by Katata (2009), respectively.

Ice content at each soil layer η_i (m^3 m^{-3}) is determined similar to snow ice content in Eq. (5) as:

$$\frac{\partial\eta_i}{\partial t} = -\frac{E_{mel}}{\rho_i}, \quad (17)$$

$$E_{mel} = \frac{C_s\rho_s}{l_f}\frac{T_s - T_m}{\partial t}, \quad (18)$$

where ρ_i is the density of ice (kg m^{-3}).

References

Ammann C., Flechard C., Leifeld J., Neftel A., Fuhrer J. (2007). The carbon budget of newly established temperate grassland depends on management intensity. Agriculture, Ecosystems & Environment, 121, 5-20.

Arora V.K., Boer G.J. (2003). A representation of variable root distribution in dynamic vegetation models. Earth Interactions, 7, 1-19.

Arora V.K., Boer G.J. (2005). A parameterization of leaf phenology for the terrestrial ecosystem

component of climate models. Global Change Biology, 11, 39-59.

Boone A. (2002). Description du schema de neige ISBA-ES (Explicit Snow). Centre National de Recherches Météorologiques, Météo-France, Toulouse. Available from: http://www.cnrm.meteo.fr/IMG/pdf/snowdoc.pdf.

Essery R., Morin S., Lejeune Y., Menard C. (2013). A comparison of 1701 snow models using observations from an alpine site. Advances in Water Resources, 55, 131-148.

Hirashima H., Yamaguchi S., Sati A., Lehning M. (2010). Numerical modeling of liquid water movement through layered snow based on new measurements of the water retention curve. Cold Regions Science and Technology, 64(2), 94-103.

Höglind M., Hanslin H.M., Mortensen L.M. (2011). Photosynthesis of Lolium perenne L. at low temperatures under low irradiances. Environmental and Experimental Botany, 70(2-3), 297-304.

Höglind M., Van Oijen M., Cameron D., Persson T. (2016). Process-based simulation of growth and overwintering of grassland using the BASGRA model. Ecological Modelling, 335, 1-15.

Jordan R. (1991). A one-dimensional temperature model for a snow cover. Technical documentation for SNTHERM.89. CRREL Special Report 91-16; US Army Core of Engineers Cold Regions Research and Engineering Laboratory, Hanover, NH, 48 pp.

Katata G. (2009). Improvement of a land surface model for accurate prediction of surface energy and water balances. JAEA-Data/Code 2008-033, JAEA, Japan, 64 pp.

126 Katata G., Kajino M., Matsuda K., Takahashi A., Nakaya K. (2014). A numerical study of the
127 effects of aerosol hygroscopic properties to dry deposition on a broad-leaved forest.
128 Atmospheric Environment, 97, 501-510.

129 Katata G., Ota M. (2017). A terrestrial ecosystem model (SOLVEG) coupled with atmospheric
130 gas and aerosol exchange processes. JAEA-Data/Code 2016-014, JAEA, Japan, 35 pp.

131 Monteith J.L. (1981). Evaporation and Surface-Temperature. Quarterly Journal of the Royal
132 Meteorological Society, 107(451), 1-27.

133 Nagai H. (2004). Atmosphere-soil-vegetation model including CO_2 exchange processes:
134 SOLVEG2, JAERI-Data/Code 2004-014, JAEA, 92 pp.

135 Oleson K.W., Lawrence D.M., Bonan G.B., Flanner M.G., Kluzek E., Lawrence P.J., Levis S.,
136 Swenson S.C., Thornton P.E. (2010). Technical description of version 4.0 of the
137 Community Land Model (CLM), NCAR Technical Note NCAR/TN-461+STR,
138 National Center for Atmospheric Research (NCAR), Boulder, CO, 257 pp.

139 Ota M., Nagai H., Koarashi J. (2013). Root and dissolved organic carbon controls on subsurface
140 soil carbon dynamics: A model approach. Journal of Geophysical Research, 118(4),
141 1646-1659.

142 Schapendonk A.H.M.C., Stol W., van Kraalingen D.W.G, Bouman B.A.M. (1998). LINGRA –
143 a source/sink model to simulate grassland productivity in Europe. European Journal of
144 Agronomy, 9(2-3), 87-100.

145 Thornley J.H.M., France J. (2007). Mathematical models in agriculture. Quantitative Methods
146 for the Plant, Animal and Ecological Sciences. 2nd Edition. Wallingford, CABI, 928 pp.

147 Van Oijen M., Höglind M., Hanslin M.H., Caldwell N. (2005). Process-based modeling of
148 timothy regrowth. Agronomy Journal, 97(5), 1295–1303.

149 Wiscombe W.J., Warren S.G. (1980). A model for the spectral albedo of snow. I: pure snow,
150 Journal of Atmospheric Science. 37, 2712-2733.

151 Yamazaki T. (2001). A one-dimensional land surface model adaptable to intensely cold regions
152 and its applications in eastern Siberia. Journal of the Meteorological Society of Japan,
153 79(6), 1107-1118.

154 Zhang X., Sun S., Xue Y. (2007). Development and testing of a frozen soil parameterization for
155 cold region studies. Journal of Hydrometeorology, 8, 690-701.

156